

---

# Analysis Plug-and-Play Methods for Imaging Inverse Problems

Edward P. Chandler<sup>1</sup> Shirin Shoushtari<sup>1</sup> Brendt Wohlberg<sup>2</sup> Ulugbek S. Kamilov<sup>1</sup>

<sup>1</sup>Washington University in St. Louis      <sup>2</sup>Los Alamos National Laboratory

{e.p.chandler, s.shirin, kamilov}@wustl.edu, brendt@ieee.com

## Abstract

Plug-and-Play Priors (PnP) is a popular framework for solving imaging inverse problems by integrating learned priors in the form of denoisers trained to remove Gaussian noise from images. In standard PnP methods, the denoiser is applied directly in the image domain, serving as an implicit prior on natural images. This paper considers an alternative *analysis* formulation of PnP, in which the prior is imposed on a transformed representation of the image, such as its gradient. Specifically, we train a Gaussian denoiser to operate in the gradient domain, rather than on the image itself. Conceptually, this is an extension of total variation (TV) regularization to learned TV regularization. To incorporate this gradient-domain prior in image reconstruction algorithms, we develop two analysis PnP algorithms based on half-quadratic splitting (APnP-HQS) and the alternating direction method of multipliers (APnP-ADMM). We evaluate our approach on image deblurring and super-resolution, demonstrating that the analysis formulation achieves performance comparable to image-domain PnP algorithms.

## 1 Introduction

Imaging inverse problems seek to estimate an image from a set of noisy measurements. A common strategy is to formulate an optimization problem that incorporates both a forward measurement model and a prior that encodes assumptions about the structure of the desired solution. In classical signal processing, handcrafted priors such as total variation (TV) have been widely used to regularize inverse problems [1]. While these hand-crafted priors can work well, they often introduce reconstruction artifacts, such as staircasing in TV-regularized solutions [2]. This limitation arises because handcrafted priors are typically too simplistic to accurately model the complex statistics of natural images.

As deep learning image priors have demonstrated superior capabilities in capturing high-dimensional data distributions, learned priors have become central to state-of-the-art solutions for imaging inverse problems [3, 4]. Plug-and-play (PnP) methods have been extensively used to incorporate such learned priors, specified by denoisers, for solving inverse problems [5, 6]. PnP methods are not only empirically successful but also supported by theoretical analyses that guarantee convergence under certain conditions [7].

Historically, an important direction for the development of image priors was the decomposition of images into transformed features, such as the image gradient [1] or wavelets [8]. While such decompositions played a central role in classical signal processing and image reconstruction, they have been largely underutilized in modern deep learning. An important framework in signal processing for incorporating these decompositions in image reconstruction is that of *analysis priors* [9, 10]. In this problem formulation, priors impose some structure, commonly sparsity, on the transformed representation of the reconstructed image. Despite their importance in classical signal processing, analysis priors have received little attention in a deep learning context. While deep learning methods are highly effective in the image domain, the success of classical decompositions motivates their re-examination in modern deep-learning settings.

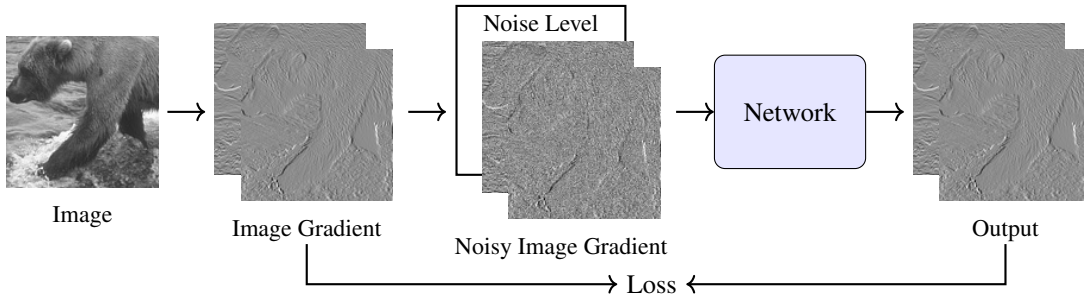


Figure 1: Training pipeline for an image gradient prior. The image gradient is computed from the image, additive white gaussian noise is added with a randomly selected noise level, the noisy gradient and noise level is passed through the network, and the output is compared to the clean image gradient via the loss.

In this work, we develop a learned image gradient prior which is incorporated within an Analysis PnP Half Quadratic Splitting (*APnP-HQS*) reconstruction algorithm and an Analysis PnP Alternating Direction Method of Multipliers (*APnP-ADMM*) reconstruction algorithm. We experimentally demonstrate the viability of such priors by showing that they can achieve similar reconstruction performance to those obtained with standard learned image priors. These results demonstrate the potential of modern deep analysis priors, such as learned image gradient priors, when used within reconstruction algorithms for image restoration.

## 2 Background

### 2.1 Imaging Inverse Problems

Many imaging systems can be formulated as

$$\mathbf{y} = \mathbf{A}\mathbf{x} + \mathbf{n}, \quad (1)$$

where  $\mathbf{A} \in \mathbb{R}^{m \times n}$  is the forward model of the imaging system,  $\mathbf{x} \in \mathbb{R}^n$  denotes the image to recover,  $\mathbf{n} \in \mathbb{R}^m$  represents noise, and  $\mathbf{y} \in \mathbb{R}^m$  is the measurement. The goal is to solve an *inverse problem*, where  $\mathbf{x}$  is recovered from  $\mathbf{y}$ . It is common to formulate the inverse problem as an optimization

$$\arg \min_{\mathbf{x}} f(\mathbf{x}) + g(\mathbf{x}), \quad (2)$$

where  $f$  is the *data-fidelity* term enforcing measurement consistency and  $g$  is the *prior* or *regularization* term that restricts the feasible solutions of  $\mathbf{x}$ . One of the most commonly used  $f$  is  $\frac{1}{2}\|\mathbf{A}\mathbf{x} - \mathbf{y}\|_2^2$ , which arises from the maximum likelihood estimation under the assumption of additive white Gaussian noise in  $\mathbf{y}$  [11]. The prior term  $g$  is meant to enforce desired features for the reconstructions. A classical example is that of total variation (TV) [1], which enforces the piecewise smoothness of images.

### 2.2 Analysis Signal Priors

The *analysis formulation* of Eq. (2) places a prior on a transformed version of  $\mathbf{x}$  [9, 10]. This transformation has historically been a linear map. Letting the linear transformation be  $\mathbf{D}$ , Eq. (2) can be written with an analysis prior as

$$\arg \min_{\mathbf{x}} f(\mathbf{x}) + g(\mathbf{D}\mathbf{x}). \quad (3)$$

Popular versions of  $\mathbf{D}$  are the image gradient and wavelet transform [1, 8], and  $g$  is commonly a sparsity-enforcing norm, such as the  $\ell_1$  norm. An example is anisotropic TV, where  $\mathbf{D}$  is the image gradient and  $g$  is the  $\ell_1$  norm:  $\|\mathbf{D}\mathbf{x}\|_1$ . The image gradient is the finite difference of the image  $\mathbf{x}$  along the horizontal and vertical axes. This can be written as the convolution along the horizontal and vertical axes of the image with the kernel  $\mathbf{d} = [1, -1]$ . In this work, we only consider the case when  $\mathbf{D}$  is the image gradient.

---

**Algorithm 1** APnP-HQS

---

**input:** forward model  $\mathbf{A}$ , measurement  $\mathbf{y}$ , gradient denoiser  $\mathcal{D}_\theta$ , image noise level  $\sigma$ , denoiser prior strength schedule  $\sigma_t$ , and regularization parameter  $\lambda$ .

- 1: Initialize  $\mathbf{x}_0$  from  $\mathbf{y}$ ; let  $\alpha_t := \lambda\sigma^2/\sigma_t^2$
- 2: **for**  $t = 1$  to  $T$  **do**
- 3:    $\mathbf{z}_t = \mathcal{D}_\theta(\mathbf{D}\mathbf{x}_{t-1}, \sigma_t)$
- 4:    $\mathbf{x}_t = \arg \min_{\mathbf{x}} \|\mathbf{A}\mathbf{x} - \mathbf{y}\|_2^2 + \alpha_t \|\mathbf{D}\mathbf{x} - \mathbf{z}_t\|_2^2$
- 5: **end for**
- 6: **return**  $\mathbf{x}_T$

---



---

**Algorithm 2** APnP-ADMM

---

**input:** forward model  $\mathbf{A}$ , measurement  $\mathbf{y}$ , gradient denoiser  $\mathcal{D}_\theta$ , image noise level  $\sigma$ , denoiser prior strength schedule  $\sigma_t$ , and regularization parameter  $\lambda$ .

- 1: Initialize  $\mathbf{x}_0$  from  $\mathbf{y}$ ; initialize  $\mathbf{s}_0$  to  $\mathbf{0}$ ; let  $\alpha_t := \lambda\sigma^2/\sigma_t^2$
- 2: **for**  $t = 1$  to  $T$  **do**
- 3:    $\mathbf{z}_t = \mathcal{D}_\theta(\mathbf{D}\mathbf{x}_{t-1} - \mathbf{s}_{t-1}, \sigma_t)$
- 4:    $\mathbf{x}_t = \arg \min_{\mathbf{x}} \|\mathbf{A}\mathbf{x} - \mathbf{y}\|_2^2 + \alpha_t \|\mathbf{z}_t + \mathbf{s}_{t-1} - \mathbf{D}\mathbf{x}\|_2^2$
- 5:    $\mathbf{s}_t = \mathbf{s}_{t-1} + \mathbf{z}_t - \mathbf{D}\mathbf{x}_t$
- 6: **end for**
- 7: **return**  $\mathbf{x}_T$

---

### 2.3 Plug-and-Play Priors

The *Plug-and-Play (PnP)* framework solves Eq. (2) by incorporating a learned prior with a data-fidelity term [6]. These priors are generally trained to be Gaussian image denoisers, although other paradigms have been explored [12–16]. An important aspect of PnP is that the prior is trained without any knowledge of the inverse problem for which it will be used, i.e. it is trained purely as an image denoiser. Therefore, the PnP framework provides a method to solve any imaging inverse problem that can be formulated as Eq. (2) without training a separate neural network for each problem.

While many PnP algorithms have been proposed, the most relevant to this paper is the algorithm based on the alternating direction method of multipliers (ADMM) [17] and DPIR [18], which uses a learned image denoiser in a half-quadratic splitting (HQS) [19] algorithm.

The vast majority of the priors used within PnP algorithms are those on the image space itself. Absent from the current literature is the development of deep neural network-based analysis priors for image reconstruction – i.e. neural networks learned to represent traditional transformed domains such as image gradients and then used within PnP algorithms.

## 3 Method

### 3.1 Image Gradient Prior

We take inspiration from the analysis problem formulation and propose incorporating a learned prior on the image gradient rather than the image itself. In particular, we learn an additive white gaussian noise (AWGN) denoiser  $\mathcal{D}_\theta$  on the image gradient. This can be interpreted as a deep learning analogue to the total variation prior.

In order to train the analysis prior network, we apply the image gradient operator  $\mathbf{D}$  to an image and add synthetic noise  $\mathbf{n}$  with variance  $\sigma^2$ . We use the  $\ell_1$  training loss

$$\|(\mathcal{D}_\theta(\mathbf{D}\mathbf{x} + \sigma\mathbf{n}, \sigma), \mathbf{D}\mathbf{x})\|_1. \tag{4}$$

The input to the network is the noisy image gradient and noise level and its output is the denoised image gradient. Figure 1 illustrates the training procedure.

### 3.2 Analysis PnP Formulation

For image reconstruction, we use the following analysis formulation:

$$\arg \min_{\mathbf{x}} f(\mathbf{x}) + \lambda\mathcal{R}(\mathbf{D}\mathbf{x}). \tag{5}$$

The prior is  $g = \lambda\mathcal{R}$ , where  $\mathcal{R}$  is the implicit regularization function of the denoiser  $\mathcal{D}_\theta$  and  $\lambda$  is a regularization strength parameter. As is standard in PnP methods, we do not have access to the function  $\mathcal{R}$  itself; it is only implicitly available through the gradient prior  $\mathcal{D}_\theta$ .

Table 1: Performance for image deblurring and super resolution comparing image-space PnP with gradient space Analysis PnP (APnP). A scale factor (SF) of 1 indicates deblurring, while scale factors 2 and 3 are for 2 $\times$  and 3 $\times$  super resolution. We report performance for noiseless and noisy measurements. Each scale factor/noise result is averaged over 8 blur kernels.

SSIM						PSNR					
SF	Noise	DPIR	APnP-HQS	PnP-ADMM	APnP-ADMM	SF	Noise	DPIR	APnP-HQS	PnP-ADMM	APnP-ADMM
1	0	0.8746	0.8711	0.8618	0.8541	1	0	31.67	31.40	31.11	30.79
	7.65	0.7447	0.7210	0.7297	0.7282	1	7.65	27.06	26.72	26.66	26.58
2	0	0.8385	0.8371	0.8329	0.8287	2	0	28.91	28.81	28.69	28.50
	7.65	0.6912	0.6689	0.6786	0.6731		7.65	25.77	25.53	25.50	25.41
3	0	0.7754	0.7740	0.7732	0.7691	3	0	27.13	27.02	26.98	26.85
	7.65	0.6501	0.6330	0.6416	0.6321		7.65	24.91	24.74	24.69	24.59

In order to solve general Eq. (5), we propose an HQS and an ADMM inspired PnP algorithm. Both of these algorithms take advantage of variable splitting. The difference of our approach with the current PnP literature is that we use a prior on a transformed image rather than the image itself. Therefore, we use the variable splitting  $\mathbf{z} = \mathbf{D}\mathbf{x}$  instead of  $\mathbf{z} = \mathbf{x}$ . This gives the constrained optimization problem

$$\arg \min_{\mathbf{x}} \frac{1}{2\sigma^2} \|\mathbf{A}\mathbf{x} - \mathbf{y}\|_2^2 + \lambda \mathcal{R}(\mathbf{z}) \quad \text{such that} \quad \mathbf{z} = \mathbf{D}\mathbf{x}. \quad (6)$$

### 3.3 Analysis PnP-HQS

To apply HQS to Eq. (6), we reformulate Eq. (6) into the following unconstrained optimization problem

$$\arg \min_{\mathbf{x}, \mathbf{z}} \frac{1}{2\sigma^2} \|\mathbf{A}\mathbf{x} - \mathbf{y}\|_2^2 + \lambda \mathcal{R}(\mathbf{z}) + \frac{\mu}{2} \|\mathbf{D}\mathbf{x} - \mathbf{z}\|_2^2. \quad (7)$$

HQS alternates between minimizing  $\mathbf{x}$  and  $\mathbf{z}$ , and so each iteration requires solving

$$\mathbf{z}_t = \arg \min_{\mathbf{z}} \lambda \mathcal{R}(\mathbf{z}) + \frac{\mu}{2} \|\mathbf{D}\mathbf{x}_{t-1} - \mathbf{z}\|_2^2 \quad (8)$$

$$\mathbf{x}_t = \arg \min_{\mathbf{x}} \frac{1}{2\sigma^2} \|\mathbf{A}\mathbf{x} - \mathbf{y}\|_2^2 + \frac{\mu}{2} \|\mathbf{D}\mathbf{x} - \mathbf{z}_t\|_2^2. \quad (9)$$

As is the standard approach in the PnP framework, line (8) can be replaced by

$$\mathcal{D}_\theta(\mathbf{D}\mathbf{x}, \sqrt{\lambda/\mu}).$$

In order for HQS to converge,  $\mu$  must be large, which requires a large number of iterations  $T$ . Therefore, following [20], we use a schedule of increasing  $\mu_t$ . Since  $\mu$  controls the prior strength for  $\mathcal{D}_\theta$ , this is equivalent to a decreasing noise schedule  $\sigma_t$ . For a complete discussion of this schedule, we refer to [18, 20]. The full APnP-HQS algorithm is shown in Algorithm 1.

### 3.4 Analysis PnP-ADMM

For the ADMM variant (APnP-ADMM), we use the following augmented Lagrangian for Eq. (6)

$$\frac{1}{2\sigma^2} \|\mathbf{A}\mathbf{x} - \mathbf{y}\|_2^2 + \lambda \mathcal{R}(\mathbf{z}) + \mu \mathbf{s}^\top (\mathbf{z} - \mathbf{D}\mathbf{x}) + \frac{\mu}{2} \|\mathbf{z} - \mathbf{D}\mathbf{x}\|_2^2. \quad (10)$$

Each iteration of ADMM requires solving

$$\mathbf{z}_t = \arg \min_{\mathbf{z}} \lambda \mathcal{R}(\mathbf{z}) + \frac{\mu}{2} \|\mathbf{z} - (\mathbf{D}\mathbf{x}_{t-1} - \mathbf{s}_{t-1})\|_2^2 \quad (11)$$

$$\begin{aligned} \mathbf{x}_t = \arg \min_{\mathbf{x}} \frac{1}{2\sigma^2} \|\mathbf{A}\mathbf{x} - \mathbf{y}\|_2^2 \\ + \frac{\mu}{2} \|(\mathbf{z}_t + \mathbf{s}_{t-1}) - \mathbf{D}\mathbf{x}\|_2^2 \end{aligned} \quad (12)$$

$$\mathbf{s}_t = \mathbf{s}_{t-1} + \mathbf{z}_t - \mathbf{D}\mathbf{x}_t. \quad (13)$$

Line (11) is again replaced by  $\mathcal{D}_\theta$  and the entire APnP-ADMM algorithm is displayed in Algorithm 2. We adopt the same noise schedule as described in APnP-HQS.

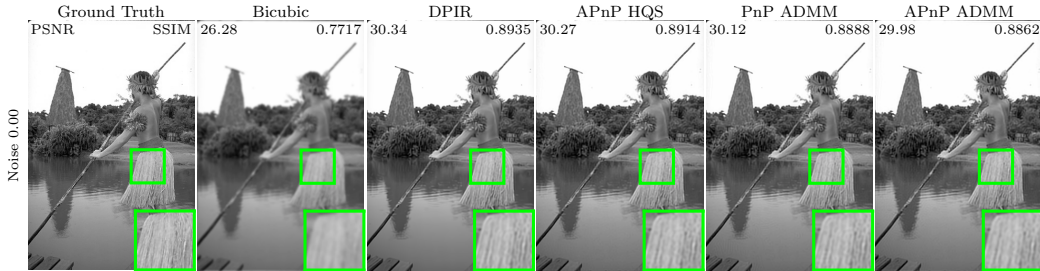


Figure 2: Visual reconstruction example of the four reconstruction algorithms for the  $2\times$  image super resolution task.

## 4 Experiments

### 4.1 Network Training

Both the image-space and gradient-space denoisers follow the DRUNet architecture [18]. In both cases, there is an extra channel for the noise level map so that the network is aware of the noise standard deviation. Therefore, the image-space network has an input of 2 channels and an output of 1 channel and the gradient-space network has an input of 3 channels and an output of 2 channels. We use the trained grayscale denoiser from [21] and trained our own image-gradient denoiser using the same natural image dataset. The images are normalized to  $[0, 1]$  by dividing each image by 255. For training, we minimize Eq. (4) with the Adam optimizer [22]. We use a batch size of 128 and crop random  $128 \times 128$  patches from the images. For each patch  $\mathbf{x}$ , the input is  $D\mathbf{x} + \sigma\mathbf{n}$  where  $\mathbf{n} \sim \mathcal{N}(0, \mathbf{I})$  and  $\sigma \sim \text{Uniform}(0, 71/255)$ . We chose this range because image-space DRUNet uses  $\sigma \sim \text{Uniform}(0, 50/255)$  and taking the image gradient of noise with variance  $\sigma^2$  results in noise with variance  $2\sigma^2$ .

### 4.2 Image Reconstruction

We test the trained priors within four PnP algorithms to solve the image deblurring and image super resolution tasks. We report results for the analysis algorithms APnP-HQS and APnP-ADMM along with their non-analysis forms DPIR and PnP-ADMM. Note that DPIR is a PnP-HQS algorithm. Following DPIR, we use 24 iterations for all algorithms and adopt the same noise schedule  $\sigma_t$ .

The forward model of the image super resolution is

$$\mathbf{y} = (\mathbf{x} \otimes \mathbf{k}) \downarrow_s + \mathbf{n},$$

where  $\mathbf{k}$  is the blurring kernel and  $\downarrow_s$  denotes downsampling by  $s$ . For image deblurring,  $s = 1$ . Following [21], we use 8 blur kernels, 4 of which are isotropic and the rest anisotropic. The fast implementation from [23] is used to solve Eq. (9) and Eq. (12) in APnP-HQS and APnP-ADMM.

Following DPIR, we use 24 iterations, adopting the same noise schedule  $\sigma_t$ ; however, for APnP-HQS we found multiplying by  $\sqrt{2}$  resulted in better performance. As reported in [18], we set  $\lambda = 0.23$  for DPIR. We empirically found  $\lambda = 0.18$  to give the best results for APnP-HQS. We used the same number of iterations and noise schedule for PnP-ADMM and APnP-ADMM. We empirically set  $\lambda = 0.38$  for PnP-ADMM and  $\lambda = 0.24$  for APnP-ADMM.

The 68 images from the BSD68 dataset [24] are used for the reconstruction experiments. As can be seen numerically and visually, the analysis versions of PnP achieve comparable performance to their standard PnP counterparts. While we generally do not outperform standard PnP, we believe our results encourage further exploration into developing analysis-based priors and architectures more suited for them. In this work we have only considered the image gradient, but other transformations, such as the wavelet transform, could result in improved analysis-based PnP algorithms.

## 5 Conclusion

In this work, we propose using an image gradient denoiser as a prior within an HQS and ADMM PnP algorithm, which we call APnP-HQS and APnP-ADMM, respectively. Empirical results show that APnP-HQS and APnP-ADMM can obtain comparable reconstructions to standard PnP. While we do not achieve state-of-the-art, this work demonstrates that analysis priors can be extended for the deep learning era. We believe further work on the variable splitting and inference algorithms can close this gap.

## References

- [1] Leonid I. Rudin, Stanley Osher, and Emad Fatemi, “Nonlinear total variation based noise removal algorithms,” *Physica D: Nonlinear Phenomena*, vol. 60, no. 1, pp. 259–268, Nov. 1992.
- [2] David Strong and Tony Chan, “Edge-preserving and scale-dependent properties of total variation regularization,” *Inverse Problems*, vol. 19, no. 6, pp. 165–187, 2003.
- [3] Ashish Bora, Ajil Jalal, Eric Price, and Alexandros G Dimakis, “Compressed sensing using generative models,” in *International Conference on Machine Learning*. PMLR, 2017, pp. 537–546.
- [4] Mojtaba Kadkhodaie and Eero P Simoncelli, “Solving linear inverse problems using the prior implicit in a denoiser,” *arXiv preprint arXiv:2007.13640*, 2020.
- [5] Singanallur V. Venkatakrishnan, Charles A. Bouman, and Brendt Wohlberg, “Plug-and-Play priors for model based reconstruction,” in *IEEE Global Conf. on Signal and Info. Proc.*, Dec. 2013, pp. 945–948.
- [6] Ulugbek S. Kamilov, Charles A. Bouman, Gregory T. Buzzard, and Brendt Wohlberg, “Plug-and-Play Methods for Integrating Physical and Learned Models in Computational Imaging: Theory, algorithms, and applications,” *IEEE Signal. Proc. Mag.*, vol. 40, no. 1, pp. 85–97, Jan. 2023.
- [7] Jiaming Liu, Yu Sun, Cihat Eldeniz, Weijie Gan, Hongyu An, and Ulugbek S. Kamilov, “Rare: Image reconstruction using deep priors learned without groundtruth,” *IEEE J. of Selected Topics in Signal Proc.*, vol. 14, no. 6, pp. 1088–1099, 2020.
- [8] S. Mallat, *A Wavelet Tool of Signal Processing: The Sparse Way*, Academic Press, San Diego, 3rd edition, 2009.
- [9] Michael Elad, Peyman Milanfar, and Ron Rubinstein, “Analysis versus synthesis in signal priors,” in *Euro. Signal Proc. Conf.*, Sept. 2006, pp. 1–5, ISSN: 2219-5491.
- [10] Ivan W. Selesnick and Mário A. T. Figueiredo, “Signal restoration with overcomplete wavelet transforms: comparison of analysis and synthesis priors,” in *Wavelets XIII*. Sept. 2009, vol. 7446, pp. 107–121, SPIE.
- [11] Stephen Boyd and Lieven Vandenbergh, *Convex Optimization*, Cambridge Univ. Press, Cambridge, 2004.
- [12] Dmitry Ulyanov, Andrea Vedaldi, and Victor Lempitsky, “Deep image prior,” in *Proc. CVPR*, June 2018.
- [13] Mauricio Delbracio and Peyman Milanfar, “Inversion by direct iteration: An alternative to denoising diffusion for image restoration,” *Trans. on Mach Learn. Research*, 2023.
- [14] Linqi Zhou, Aaron Lou, Samar Khanna, and Stefano Ermon, “Denoising diffusion bridge models,” in *Proc. ICLR*, 2024.
- [15] Y. Hu, A. Peng, W. Gan, P. Milanfar, M. Delbracio, and U. S. Kamilov, “Stochastic deep restoration priors for imaging inverse problems,” 2024, arXiv:2410.02057.
- [16] Matthieu Terris, Ulugbek S Kamilov, and Thomas Moreau, “Fire: Fixed-points of restoration priors for solving inverse problems,” in *Proc. CVPR*, 2025, pp. 23185–23194.
- [17] Stephen Boyd, Neal Parikh, Eric Chu, Borja Peleato, and Jonathan Eckstein, “Distributed optimization and statistical learning via the alternating direction method of multipliers,” *Found. and Trends in Mach. Learn.*, vol. 3, no. 1, pp. 1–122, 2011.
- [18] Kai Zhang, Yawei Li, Wangmeng Zuo, Lei Zhang, Luc Van Gool, and Radu Timofte, “Plug-and-Play Image Restoration With Deep Denoiser Prior,” *IEEE Trans. PAMI*, vol. 44, no. 10, pp. 6360–6376, Oct. 2022.
- [19] D. Geman and Chengda Yang, “Nonlinear image recovery with half-quadratic regularization,” *IEEE Trans. Image Proc.*, vol. 4, no. 7, pp. 932–946, July 1995.
- [20] Kai Zhang, Wangmeng Zuo, Shuhang Gu, and Lei Zhang, “Learning Deep CNN Denoiser Prior for Image Restoration,” in *Proc. CVPR*, July 2017, pp. 2808–2817, ISSN: 1063-6919.
- [21] Kai Zhang, Luc Van Gool, and Radu Timofte, “Deep Unfolding Network for Image Super-Resolution,” in *Proc. CVPR*, June 2020, pp. 3214–3223, ISSN: 2575-7075.

- [22] Diederick P Kingma and Jimmy Ba, “Adam: A method for stochastic optimization,” in *Proc. ICLR*, 2015.
- [23] Ningning Zhao, Qi Wei, Adrian Basarab, Nicolas Dobigeon, Denis Kouame, and Jean-Yves Tournet, “Fast Single Image Super-Resolution Using a New Analytical Solution for l2 - l2 Problems,” *IEEE Trans. Image Proc.*, vol. 25, no. 8, pp. 3683–3697, Aug. 2016.
- [24] D. Martin, C. Fowlkes, D. Tal, and J. Malik, “A database of human segmented natural images and its application to evaluating segmentation algorithms and measuring ecological statistics,” in *Proc. ICCV*, 2001, vol. 2, pp. 416–423 vol.2.